



# HHS Public Access

Author manuscript

*Exp Neurol.* Author manuscript; available in PMC 2016 July 01.

Published in final edited form as:

*Exp Neurol.* 2015 July ; 269: 120–132. doi:10.1016/j.expneurol.2015.04.001.

## Seizure Reduction through Interneuron-mediated Entrainment using Low Frequency Optical Stimulation

Thomas P. Ladas, Chia-Chu Chiang, Luis E. Gonzalez-Reyes, Theodore Nowak, and Dominique M. Durand

Department of Biomedical Engineering, Neural Engineering Center, Case Western Reserve University, Cleveland OH 44106, USA

### Abstract

Low frequency electrical stimulation (LFS) can reduce neural excitability and suppress seizures in animals and patients with epilepsy. However the therapeutic outcome could benefit from the determination of the cell types involved in seizure suppression. We used optogenetic techniques to investigate the role of interneurons in LFS (1Hz) in the epileptogenic hippocampus. Optical low frequency stimulation (oLFS) was first used to activate the cation channel channelrhodopsin-2 (ChR2) in the Thy1-ChR2 transgenic mouse that expresses ChR2 in both excitatory and inhibitory neurons. We found that oLFS could effectively reduce epileptiform activity in the hippocampus through the activation of GAD-expressing hippocampal interneurons. This was confirmed using the VGAT-ChR2 transgenic mouse, allowing for selective optical activation of only GABA interneurons. Activating hippocampal interneurons through oLFS was found to cause entrainment of neural activity similar to electrical stimulation, but through a GABA<sub>A</sub>-mediated mechanism. These results confirm the robustness of the LFS paradigm and indicate that GABA interneurons play an unexpected role of shaping inter-ictal activity to decrease neural excitability in the hippocampus.

### Keywords

Optogenetics; Mesial temporal lobe epilepsy; Low-frequency stimulation; Seizure suppression; GABA interneuron

### Introduction

Epilepsy is a chronic disorder of the central nervous system characterized by recurrent, unprovoked seizures. Mesial temporal lobe epilepsy (MTLE) involving the hippocampus is a common type of epilepsy, often medically refractory and necessitating surgical resection if

© 2015 Published by Elsevier Inc.

Corresponding author: Dominique M. Durand, Departments of Biomedical Engineering, Neurosciences, and Physiology & Biophysics, Case Western Reserve University, 10900 Euclid Ave, Wickenden Bldg. Rm. 112, Cleveland, OH 44106, Business: 216.368.3974, Facsimile: 216.368.4872, dominique.durand@case.edu.

**Publisher's Disclaimer:** This is a PDF file of an unedited manuscript that has been accepted for publication. As a service to our customers we are providing this early version of the manuscript. The manuscript will undergo copyediting, typesetting, and review of the resulting proof before it is published in its final citable form. Please note that during the production process errors may be discovered which could affect the content, and all legal disclaimers that apply to the journal pertain.

an epileptic focus can be identified (Wiebe *et al.*, 2001). A less invasive alternative to surgery shown to reduce disease burden is deep brain electrical stimulation (DBS) (Fisher *et al.*, 2010; Jobst *et al.*, 2010; Morrell, 2011), although the optimal location and stimulus paradigm is highly debated and the mechanisms of seizure suppression remain poorly understood (Sunderam *et al.*, 2010). Nonetheless, recent studies have shown low frequency electrical stimulation to be effective at suppressing epileptiform activity in animal models (Rashid *et al.*, 2012) and reducing seizure frequency in patients (Koubeissi *et al.*, 2013).

Despite the advantages offered by a low frequency electrical treatment strategy, the inherent lack of cell type-specificity in using an electrical stimulus to modulate neuronal activity may limit overall efficacy and create undesired side effects. The confounding effects from non-specific cell activation also make it difficult to determine the mechanisms responsible for the therapeutic effect. There is much debate over whether stimulation of the neurons at the seizure focus (Bragin *et al.*, 2002), afferent connections (Yang *et al.*, 2006), or even local glial cells (Tawfik *et al.*, 2010) are important for reducing seizure activity. The emerging field of optogenetics can help address these questions by providing tools that allow for cell-specific activation (Boyden *et al.*, 2005) or inhibition (Zhang *et al.*, 2007; Chow *et al.*, 2010) in a reversible manner with millisecond time resolution. These optogenetic constructs have recently been shown to suppress neuronal hyperactivity and seizure in various models epilepsy (Paz *et al.*, 2012; Wykes *et al.*, 2012; Krook-Magnuson *et al.*, 2013) but can also be applied to elucidate the mechanisms seizure suppression.

In the present study, we used optogenetic techniques to investigate the role of interneurons in low-frequency stimulation paradigms that have been shown to suppress epileptiform activity in the hippocampus (Rashid *et al.*, 2012; Koubeissi *et al.*, 2013). Two different optogenetic transgenic mouse models expressing ChR2 were used to study the effects of selectively activating hippocampal neurons or only GABA interneurons to assess the role these cell types play in suppressing seizure activity. The pro-epileptogenic compound 4-aminopyridine (4-AP) was used as a model of epilepsy (Perreault and Avoli, 1989) in both *in vitro* (Zhang *et al.*, 2014) and acute *in vivo* (Gonzalez-Reyes *et al.*, 2013) preparations. This compound has been shown to trigger epileptiform activity *in vivo* after local (intra-hippocampal) (Gonzalez-Reyes *et al.*, 2013) and systemic (Levesque *et al.*, 2013) administration. While this work was primarily aimed to gain insight into the mechanisms of seizure reduction using LFS, the efficacy of this approach *in vivo* adds to the growing body of evidence that translation of optogenetic techniques can provide more targeted therapy for future clinical applications.

## Materials and methods

### Animals

Thy1-ChR2-YFP (B6.Cg-Tg(Thy1-COP4/EYFP)9Gfng/J Stock Number:007615) and VGAT-ChR2-YFP (B6.Cg-Tg(Slc32a1-COP4\*H134R/EYFP)8Gfng/J Stock Number: 014548) transgenic mice (both of C57BL/6 background) were bred from founder animals obtained from the Jackson Laboratory. We used these two transgenic animals since the promoters Thy-1 (Arenkiel *et al.*, 2007) and VGAT (Zhao *et al.*, 2011) control the expression of the ChR2 opsin only in neurons and in GABAergic cells, respectively.

Animals were housed no more than 5 adult animals per cage and maintained in a SPF room under light (12-h light/12-h dark cycle), temperature and humidity controlled conditions. Animals used for *in vitro* brain slice experiments were studied at approximately postnatal day 14 (P14, range P11 to P16) and P90. For acute *in vivo* experiments, adult animals were used (range P90 to P110). Both male and female animals were used for experiments as no differences due to animal gender were observed. All experimental procedures performed in this study followed the NIH animal use guidelines and were approved by the Institutional Animal Care and Use Committee (IACUC) at Case Western Reserve University.

## Histology

Transgenic and wildtype mice from both mouse lines were transcardially perfused with ice-cold 4% paraformaldehyde (PFA) under isoflurane anesthesia at age P14 and P100. Brains were then removed, post-fixed in 4% PFA at 4°C overnight, and cryoprotected in 30% sucrose in phosphate-buffered saline (PBS) for 2 days before being flash-frozen in 2-methylbutane on dry ice and stored at -80°C. Brains were then sectioned at a thickness of 40 µm using a cryostat (Leica CM3050S), and free-floating sections were blocked in 5% horse serum for 1hr then stained for GAD-67 (rabbit, Santa Cruz (sc-5602), 1:100 dilution) or GAD-65/67 (rabbit, ABCam (ab49832), 1:1000 dilution) at 4°C overnight. Sections were then incubated with secondary antibodies conjugated to Cy3 (donkey α-rabbit, 1:700, Jackson ImmunoResearch, West Grove, PA). After rinsing in PBS, sections were mounted on Fisherbrand Superfrost/Plus microscope slides in VECTASHIELD mounting media (Vector Laboratories, Burlingame, CA). For 40 µm sections, TOTO-3 (1:2000 dilution, Invitrogen) was included to visualize nuclei and confocal microscopy was used to capture Z-stacked images on a Zeiss LSM 510 META laser-scanning microscope. All YFP- and GAD-positive neurons in the hippocampus that could be identified were counted from n=6 transgenic (P14, n=3; P100, n=3) and n=2 wildtype mice from each mouse line. Immunohistochemical images presented represent a typical IHC staining result.

## Acute *in vivo* recording and optical stimulation

Adult transgenic and wildtype mice were anesthetized with isoflurane and mounted to a stereotaxic frame (Stoelting, Wood Dale, IL). Anesthesia was maintained throughout the stereotaxic surgery by delivering 3% isoflurane in a carbogen gas mixture (95% O<sub>2</sub>/5% CO<sub>2</sub>) via a constant pressure mask, and depth of anesthesia was assessed by monitoring animal respiratory rate and response to toe pinch. Screw electrodes were placed in the skull for use as the reference (positioned caudally in the occipital bone) and system ground (positioned rostrally in the frontal/coronal bones). Depth electrodes (tungsten, A-M Systems) were positioned in the septal CA3 region of the hippocampus bilaterally (bregma -1.7 mm, lateral ±2.0 mm, depth 2.1 mm). Local field potential neural activity was bandpass filtered (1 Hz to 5 kHz) and amplified (gain of 1000, A-M Systems Model 1700 Differential AC Amplifier), then digitized at 20 kHz (PowerLabs/16SP) using LabChart7 software (ADInstruments, Dunedin, New Zealand) and stored for off-line analysis. Epileptiform activity was induced by 1 µL bolus injections of 40 mM 4-AP (in nACSF) in the left septal CA3 region (bregma -1.8 mm, lateral 2.0 mm, depth 2.1 mm). Additional injections were administered every 10 minutes until the development of sustained electrographic seizure activity for the duration of the experiment, with an average dose of 3±1 µL. The resultant

electrographic seizure was self-sustained for the duration of the experiment. A stripped and freshly cleaved optical fiber (0.48 NA, 200  $\mu\text{m}$  diameter, Thorlabs) was placed at the site of 4-AP injection, positioned at a 30° angle to maximally illuminate the dorsal hippocampus. Optical patch chords were connected to a 100 mW 473 nm fiber-coupled DPSS laser (OEM Laser Systems, Bluffdale, UT) controlled by a TTL trigger source provided by the digital acquisition system that was programmed to output 1 Hz pulse trains with 5 ms pulse width. The laser power applied to the tissue during 1 Hz optical pulse trains was measured to be  $\sim 11 \text{ mW/mm}^2$ .

### Brain slice electrophysiology

Transgenic and wildtype mice were decapitated under isoflurane anesthesia and the brains were rapidly removed and placed in ice-cold high-sucrose artificial cerebrospinal fluid (S-aCSF) containing (in mM): sucrose, 75; NaCl, 85; KCl, 2.5;  $\text{NaH}_2\text{PO}_4$ , 1.25;  $\text{NaHCO}_3$ , 25; D-glucose, 25;  $\text{MgCl}_2$ , 4;  $\text{CaCl}_2$ , 0.5; and bubbled with a 95%  $\text{O}_2$ /5%  $\text{CO}_2$  gas mixture. After fixing the whole brain to a cutting block using cyanoacrylate glue, 350  $\mu\text{m}$  transverse hippocampal slices were cut in S-aCSF at low temperature using a vibratome (VT1000S, Leica, Nusslock, Germany) and placed in a bubbled storage solution at room temperature containing (in mM): NaCl, 125; KCl, 2.5;  $\text{NaH}_2\text{PO}_4$ , 1.25; D-glucose, 25;  $\text{NaHCO}_3$ , 25;  $\text{MgCl}_2$ , 4;  $\text{CaCl}_2$ , 1. After a one hour incubation, slices were transferred to a bath-immersion recording chamber (Warner Instruments, Hamden, CT) and superfused with gas-bubbled normal aCSF heated to 32°C containing (in mM): NaCl, 125, KCl, 2.5;  $\text{NaH}_2\text{PO}_4$ , 1.25; D-glucose, 25,  $\text{NaHCO}_3$ , 25;  $\text{MgCl}_2$ , 2;  $\text{CaCl}_2$ , 2; with pH 7.6 and osmolarity 315 mOsm. Glass pipette recording electrodes were pulled from borosilicate capillary glass using a Flaming/Brown type puller (P-1000, Sutter Instruments, Novato, CA) to a resistance of 5 M $\Omega$  for electrodes used to measure field potentials (150 mM NaCl pipette filling solution) or for patch clamp recordings (used for Thy1 slice experiments) or to a resistance of 90–120 M $\Omega$  for intracellular recording electrodes (4M K-Acetate filling solution, used for VGAT slice experiments). Intracellular recording techniques were used for the VGAT experiments due to the prolonged recording times and the need for an accurate measure of the membrane voltage to calculate the optical response reversal potential. A tungsten electrode (A-M Systems) was placed in the Schaffer collateral tract and used to deliver a 200–400  $\mu\text{A}$  regulated current cathodic pulse for 100  $\mu\text{s}$  (Model 2300 Digital Stimulus Isolator, A-M Systems, Carlsborg, WA) to elicit an evoked potential measured in the CA3 pyramidal cell layer in order to assess hippocampal network function and tissue viability throughout the experiment. Brain slices and electrode placements were visualized using an AxioCam MRm CCD camera on an Axioscope FS microscope (Carl Zeiss, Oberkochen, Germany) positioned above the bath recording chamber. Optical stimulation of cells expressing ChR2-YFP was done using a fiber-coupled 100 mW 473 nm DPSS laser (OEM Laser Systems, Bluffdale, UT), with the fiber bare end (200  $\mu\text{m}$  diameter) placed directly over the CA3 region in the bath. The optical stimulus area was visualized using the microscope and camera, and the position of the fiber was adjusted to obtain adequate coverage of the CA3 pyramidal cell area. Recordings were acquired using Axopatch 200B Patch Clamp Amplifier (Molecular Devices) and IE-210 Intracellular Electrometer (Warner Instruments) high impedance amplifiers and low-pass filtered at 2 kHz before being digitized at 10 kHz (Digidata 1440A, Molecular Devices) and stored for off-line analysis.

Epileptiform activity was induced by bath application of 100  $\mu\text{M}$  4-aminopyridine (4-AP, Sigma). Inhibition of GABA<sub>A</sub>-mediated processes was accomplished by adding 100  $\mu\text{M}$  picrotoxin (PTX, Sigma) to the superfused aCSF. Current-clamp pulse stimulation was applied to cells to monitor the membrane response to optical stimulation and calculate the reversal potential. Cells were injected with 500 ms pulses from  $-0.6$  nA to  $+0.6$  nA and a 10 ms optical pulse applied at  $t=400$ ms. Amplitude of the optical response was measured as the maximum or minimum voltage subtracted from the average pre-stimulus membrane voltage. Optical stimulation of wild-type control animals did not elicit any optical response and had no effect on epileptiform activity in the hippocampal slice when applied at 1Hz.

### Data Analysis and Statistics

Data were analyzed off-line using the Matlab (MathWorks, Natick, MA) and IGOR Pro (WaveMetrics, Portland, OR) software packages to create custom analysis procedures. Neuromatic procedures (J. Rothman, <http://www.neuromatic.thinkran-dom.com>) run in IGOR Pro 6.22 were used to import pCLAMP data for further analysis. For *in vivo* recordings, stimulation artifacts were first removed using a signal processing algorithm that calculated an ensemble average of all artifacts in a recording to create a template that was then subtracted from the raw data (Chiang *et al.*, 2012). With stimulation artifacts removed, the root mean square (RMS) voltage for each recording epoch was calculated as a measure of the signal power. Suppression ratios (SR) were then calculated for each stimulation period as  $SR = 100 \times (P_{baseline} - P_{stim}) / P_{baseline}$  such that a SR of zero indicates no change in signal power during stimulation and SR of 100 indicates a reduction of signal power to zero during the stimulus period. For *in vitro* experiments, only slices yielding an orthodromic population spike  $\geq 1$  mV from Schaffer collateral stimulation were used for data analysis. After the experiment, intracellular microelectrodes were withdrawn to measure the potential outside the cell, which was then subtracted from the raw data to obtain the transmembrane potential.

Statistical analysis was done using two-tailed paired *t*-test for *in vivo* experimental results to compare signal power reduction due to optical stimulation and two-tailed two-sample *t*-test to compare the calculated suppression ratios between transgenic mouse lines. For *in vitro* experiments, one-way ANOVA was used for multiple comparisons of means to assess statistical significance in the change in membrane voltage due to optical stimulation, followed by post-hoc Tukey HSD for pair-wise comparisons. Two-tailed, two-sample *t*-test was used to compare the reversal potential under normal and 4-AP conditions. Kolmogorov-Smirnov test was used to assess statistical significance of the change in the distribution of AP spiking behavior due to optical stimulation. Normality tests were run on all data sets and adjustments were made when the variance between groups compared was not similar. A statistical significance criterion of  $\alpha = 0.05$  used for all tests. Power analysis was performed on preliminary data to ensure an adequate sample size for these experiments. Results are shown as mean  $\pm$  the standard error of the mean (SEM) unless otherwise noted. In box-and-whisker plots, boxes represent the 25<sup>th</sup> percentile, median value, and 75<sup>th</sup> percentile of the data, and whiskers represent the 10<sup>th</sup> and 90<sup>th</sup> percentiles.

## Results

### Optical LFS can suppress epileptiform activity in the hippocampus *in vivo*

LFS applied electrically to the ventral hippocampal commissure in rats can suppress 90% of the seizures by activating both hippocampi (Rashid *et al.*, 2012). To determine if direct oLFS in the hippocampus could reproduce a similar seizure suppression effect, we first applied oLFS in Thy1-ChR2-YFP mice (Arenkiel *et al.*, 2007) where both excitatory and inhibitory neurons would be optically activated, as with electrical stimuli. Since the efficacy of an optical stimulus applied to suppress seizure activity was yet unknown, these experiments also served as an important baseline for later studies in interneuron-specific models. We injected 40mM 4-aminopyridine (4-AP) into the hippocampus of adult Thy1 mice under anesthesia to induce epileptiform activity. We then optically stimulated the CA3 region with 5 ms pulses at 1Hz using a 200 $\mu$ m diameter optical fiber positioned near the injection site (see Fig. 1A, B). The development of electrographic seizure in the hippocampus was monitored both ipsilaterally near the 4-AP-affected area and in the contralateral CA3 location (Fig. 1C, D). Once sustained electrographic seizure was established, stimulus trains of 1Hz optical pulses were applied for 2 minutes (Fig. 1C, blue bar). Signal power before, during, and after stimulation was measured and seizure suppression was calculated to quantify the effect of stimulation on epileptiform activity (Fig. 2). Seizure activity during the stimulation period was suppressed (see Fig. 1C, F) by  $68\pm 8\%$  ( $n=7$ ,  $P<0.001$ ) after 120s of 1Hz oLFS (Fig. 2B). Following the stimulation period (Fig. 1G), a reduction of hippocampal hyperactivity persisted on the ipsilateral side (Fig. 2B,  $51\pm 7\%$  reduction as compared to before stimulation,  $n=7$ ,  $P<0.001$ ). Although 4-AP injection and optical stimulation was unilateral, abnormal neural activity quickly developed bilaterally, and contralateral epileptiform activity was also optically suppressed significantly with sustained 1Hz stimulation by  $59\pm 14\%$  after 120s of 1Hz stimulation and by  $36\pm 17\%$  that persisted after stimulation (Fig. 2B,  $n=7$ ,  $P<0.05$ ).

### Pyramidal cells respond to optical stimuli with an excitation-inhibition sequence

To further investigate the behavior of hippocampal pyramidal neurons during optical stimulation, we monitored the CA3 pyramidal cell response to optical stimulation in acute brain slices from juvenile Thy1-ChR2-YFP animals. Cells were held at  $I=0$  in current clamp mode while pulses of light were applied specifically to the CA3 region of the hippocampus using a 200 $\mu$ m diameter optical fiber placed over the tissue preparation (Fig. 3A, B). Stimulation for pulse durations of 10 ms, 20 ms, and 30 ms was applied while neuronal response was monitored (Fig. 3C–F). As would be expected from activating a cation channel, optical stimulation caused membrane depolarization and elicited action potential firing in some cells, with longer pulse durations prolonging membrane depolarization that lead to additional neuronal firing (22.2% of optically-responsive cells from  $n=18$  cells, Fig. 3C). A minority of pyramidal neurons exhibited a depolarization response to optical stimuli that did not reach threshold to fire for any pulse-width (16.7% of  $n=18$  cells, Fig. 3D). It was possible to elicit optically-evoked action potentials from these cells if a small holding current was applied to depolarize the cell (data not shown). Most optical responses, however, were typical of processes involving GABA<sub>A</sub> in the hippocampus, with a complex excitation-inhibition response or a pure hyperpolarization response (61.1% of  $n=18$  cells,

Fig. 3E, F). It was not clear, however, if this was due to feed-back inhibition or direct activation of GABA interneurons.

### ChR2-YFP expression is predominant in GABA interneurons in the hippocampus of Thy1-ChR2 transgenic mice

The complex single-cell responses to optical stimuli indicated that ChR2 expression driven on the Thy1 promoter was likely not uniformly expressed in the pyramidal cells and interneurons in the hippocampus, prompting an immunohistochemical analysis to determine the cell-types of the ChR2-expressing cells. Since the majority of cells in the hippocampus are excitatory pyramidal neurons (Woodson *et al.*, 1989) that could be easily identified by location and cell morphology, we labeled hippocampal interneurons to simplify the subsequent YFP co-localization. Frozen brain sections from Thy1-ChR2-YFP mice at age P14 and P100 were stained for the GABA-synthesizing enzyme GAD-67 (glutamate decarboxylase). The localization of histological elements is shown in a diagram depicting the transverse view of the hippocampus (Fig. 4A). The corresponding panoramic (Fig. 4B) and higher magnification (Fig. 4C) views of the CA3 region show the double labeled GABA neurons captured by triple channel confocal microscopy pictures. A separated visualization of each channel shows the red GAD-67-positive signal (Fig. 4D), the green YFP-ChR2 signal (Fig. 4E) and the blue nuclear signal (Fig. 4F) in the CA3 hippocampal region. We observed GAD-67-positive cells in and around the pyramidal cell layer, most of which also highly expressed YFP (Fig. 4D, E, arrowheads). While there were many densely packed pyramidal neurons in the hippocampus (Fig. 4F), there were relatively few YFP-positive cells overall and most co-labeled for GAD-67, indicating that ChR2-YFP expression in the CA3 region of the Thy1-ChR2-YFP mouse is predominantly in interneurons. In addition to identifying the neurons expressing ChR2-YFP, we also investigated whether ChR2 was expressed in hippocampal glial cells to rule out activation of these non-neuronal cell types. Staining for the astrocyte marker GFAP and the oligodendrocyte marker OSP in Thy1-ChR2-YFP brain sections showed that neither of these markers co-expressed with YFP (data not shown), indicating that ChR2 was not expressed in hippocampal glial cells and was therefore restricted to neurons in these mice.

To address our initial question of the role of interneurons in oLFS suppression, we next studied the VGAT-ChR2-YFP transgenic mouse (Zhao *et al.*, 2011), where ChR2 expression is driven by a GABA interneuron-specific promoter. Histological characterization of these mice (Fig. 5) revealed that  $89\pm 4\%$  of counted cells in CA3 and  $83\pm 4\%$  of cells in CA1 co-labeled for YFP and GAD-65/67 (Fig. 5G–L and **chart bottom right**). A minority of cells ( $11\pm 1\%$  and  $15\pm 4\%$  in CA3 and CA1, respectively) were found to be GABAergic but did not express ChR2-YFP, indicating that some interneurons did not express ChR2 and therefore would not be optically activated. No cells were found to express YFP and be negative for GAD-65 or GAD-67 (Fig. 5, chart bottom right). For comparison, the same quantitation in Thy1 mice found that in CA3 the majority of YFP-expressing cells co-expressed GAD-65 or GAD-67 ( $81\pm 4\%$ ), while some cells ( $12\pm 1\%$ ) were found to solely express YFP (Fig 5A–F and chart bottom left). These cells were located within the cell layer, indicating expression in pyramidal cells (Fig. 5C–F). A small number of cells ( $5\pm 1\%$ ) were found to express GAD-65/67 but not YFP. In the CA1 region, a majority of cells co-

expressed YFP and GAD-65/67 (54±3%), although some YFP-positive pyramidal cells (5±1%) were identified (Fig. 5, chart bottom left)

### Pattern of expression of Chr2-YFP at P14 and P100 in VGAT mice

We counted cells in P14 (n=3) and P100 (n=3) in VGAT mice and estimated the density of each cell type in the CA3 region (Fig. 5H–I). We did not find YFP-positive cells that morphologically appeared to be principal cells. The number of YFP positive cells that co-expressed GAD 65–67 and morphologically appeared to be interneurons was comparable at both ages (21701±249 cells/mm<sup>3</sup> from P14, and 22669±421 cells/mm<sup>3</sup> from P100, P>0.05). A similar pattern of expression was observed in the Thy1-ChR2-YFP line (Chiang *et al.*, 2014). This data show that the pattern of expression of Chr2 in GABA neurons was similar at P14 and P100 suggesting that the activation of the VGAT promoter occurs at very early time during development and is consistently maintained during adulthood.

### Optical stimulation of interneurons at 1Hz during inter-ictal behavior entrains network activity and cell firing

Given the histologic results, the initial seizure suppression studies in Thy1-ChR2 mice provided strong evidence that stimulation of interneurons may play a large role in oLFS suppression. Although found to be few in number, activation of pyramidal cells directly may still be responsible for the observed effect, especially given the high interconnectivity in the hippocampus. To confirm the optical stimulation of only GABA interneurons during oLFS suppression paradigms, we next set out to suppress epileptiform activity in acute brain slices from adult VGAT mice (P90) and juvenile VGAT mice (P14–16). Hippocampal slices exhibiting epileptiform activity from bath application of 100 μM 4-AP were optically stimulated with 10 ms pulses at 1Hz for 15 s, causing a significant reduction of interictal-like activity during the period of stimulation (frequency, pre-stimulation: 13.9±2.0 spikes/15s; during stimulation: 4.9±1.2 spikes/15s) (Fig. 6A, n=18, P<0.001). We also found the neural response to optical pulse in adult and juvenile VGAT mice is similar (Fig 6Ai, B).

Therefore, we further focused on studying pyramidal cell behavior during optical stimulation by means of both field potential and sharp electrode recordings in juvenile VGAT slices. While spontaneous inter-ictal activity occurred at a rate of 0.3 Hz to 0.5 Hz, an evoked network burst was elicited for every optical pulse during stimulation trials (n=14, Fig. 6B). Pyramidal cell activity closely followed the optical stimulus pulse train, with an action potential burst occurring after each optical pulse (Fig. 6B, ii). This phenomenon was identical to what we found in the electrically stimulated brain slices in the mossy fiber region with a 1Hz electrical LFS paradigm. (n=6, Fig. 7A–C). To assess the variability in cell membrane potential before and during stimulation trials, we measured the maximum change in cell voltage before (Fig. 6B, iii, open circles) and after (closed circles) each AP burst that correlated with a field potential discharge ( $V_m$ , see diagram in Fig. 6C). Spontaneous AP bursts were characterized by a large and variable swing in membrane voltage (mean ± SD was 13.8±5.0 mV, n=2052 events from 13 cells) with multiple spikes and slow depolarization before the next inter-ictal discharge. Optically-evoked bursting at 1Hz, however, caused pyramidal cell voltage to remain near the level of maximum hyperpolarization (Fig. 6D). Interestingly, 1Hz electrical stimulation trials produced a nearly



identical field potential and cellular response (Fig. 6D). As a result, the change in membrane voltage during optical stimulation trials was much smaller as compared to during spontaneous activity (Fig. 6E,  $1.7 \pm 0.9$  mV,  $n=214$ ,  $P<0.001$ ) and similarly the change in membrane voltage during electrical stimulation trials was measured as  $2.4 \pm 0.7$  mV (Fig. 6E,  $n=84$ ,  $P<0.001$ ).

In addition to monitoring changes in membrane potential induced by optical and electrical LFS, we also examined action potential firing during spontaneous events and 15s stimulation trials (Fig. 6F and Fig. 7D–G). For spontaneous events, cells fired action potentials with increasing frequency after the initial AP burst until the next inter-ictal discharge. Action potential bursts induced by optical stimulation exhibited high regularity between pulses ( $n=214$  burst events from 8 pyramidal cells) and showed a complete lack of additional AP firing beyond the initial burst, as did those elicited by electrical stimulation (see Fig. 7D–E). Given the lack of an external trigger for spontaneous events, AP latencies were measured from the onset of the field potential inter-ictal discharge to the cellular AP response. The distribution of AP latencies was narrower and closer to zero for optically- and electrically-evoked events as compared to spontaneous events [Fig. 6F, AP latency mean  $\pm$  SD for 4-AP spontaneous events was  $0.97 \pm 1.3$  s ( $n=14,487$ ); for optical stimulation was  $0.036 \pm 0.03$  s ( $n=904$ ) and for electrical stimulation was  $0.035 \pm 0.04$  s ( $n=228$ ),  $P<0.001$ ]. Regularly evoking these interictal-like events led to the inhibition of any extraneous pyramidal cell activity, thus shaping or “sculpting” the inter-ictal period to an overall reduced activity state. A two-sample Kolmogorov-Smirnov test was used to compare the distributions of AP firing times, confirming that optical and electrical LFS significantly changed the cell AP firing behavior (Fig. 7F,  $P<0.001$ ). The AP firing histogram highlights cell firing behavior during the initial burst event and shows that both optical and electrical stimulation produced similar burst responses (Fig. 7G).

### **Optical activation of GABA interneurons causes pyramidal cell inhibition in normal aCSF and burst firing in pro-epileptogenic conditions**

To explore how excitation of GABA interneurons could cause entrainment of pyramidal cells, we characterized the response of pyramidal cells to GABA interneurons in the normal condition and in the pro-epileptogenic condition in hippocampal slices from juvenile VGAT mice. Long-pulse stimuli (1s) were used to ensure the pyramidal cell being monitored was sufficiently innervated by ChR2-expressing interneurons. When membrane potential was approximately  $-50$  mV (either spontaneously or clamped), spontaneous firing was completely inhibited by the optical stimulus (Fig. 8A) and cell potential was hyperpolarized by  $8.1 \pm 0.4$  mV ( $n=27$ ,  $P<0.001$ ) for the duration of the pulse (Fig. 8B). Though membrane potential did fluctuate during the applied stimulus, there was no significant difference between the magnitudes of the initial and late hyperpolarization responses ( $P=0.87$ ), and cell membrane potential fully recovered to pre-pulse levels within 1s after the pulse. In order to determine the reversal potential of the optical stimulus response, a current clamp pulse protocol was performed during which a 10 ms optical pulse was applied. The amplitude of the resulting response was measured and plotted against membrane potential (Fig. 8C, D). We estimated the reversal potential of optical responses to be  $-63.3 \pm 0.7$  mV ( $n=23$ ), which is consistent with what others have reported for GABA<sub>A</sub>-induced inhibitory post-synaptic

potentials (IPSPs) (Ben-Ari *et al.*, 1989). Furthermore, the optical response was nearly completely eliminated after application of the GABA<sub>A</sub>-blocker picrotoxin (PTX, n=5), confirming that the observed pyramidal cell response was in fact due to GABA<sub>A</sub> signaling.

Bath application of 100 μM 4-AP caused spontaneous network activity typical of inter-ictal bursting behavior (Perreault and Avoli, 1989). In contrast to normal aCSF, optical stimuli applied in pro-epileptogenic conditions consistently caused pyramidal cell depolarization and AP bursting (Fig. 9A, B). A large field potential response was generated by optical stimulation, indicating that many pyramidal neurons were driven to fire simultaneously in the presence of 4-AP (n=39, Fig. 9B). To test if a chloride reversal mechanism was causing an excitatory response to GABA, current-clamp pulse stimulation with a concurrent optical stimulus was performed to determine the reversal potential in the 4-AP condition. We observed a consistently large membrane response elicited by optical stimulation. A 10 ms optical stimulus could either depolarize or hyperpolarize the membrane potential depending on the resting membrane potential (Fig. 9C, D). The reversal potential of this initial optical response was measured to be  $-64.9 \pm 1.9$  mV (n=16) and was not statistically different from the reversal potential measured in normal aCSF (P=0.76, Fig. 9E). Therefore, we concluded there is no shift of the chloride reversal potential in the pro-epileptogenic condition, and that depolarization in response to GABA stimulation was due to the lowered resting membrane potentials

### Optical LFS suppresses *in vivo* seizure activity similarly in both mouse lines

To determine if 1Hz activation of interneurons alone could suppress seizure activity *in vivo*, we repeated the 1Hz optical suppression experiments in adult VGAT-ChR2-YFP transgenic mice. Optical stimulation of hippocampal interneurons at 1Hz rapidly led to reduced hyperactivity in both the ipsilateral and contralateral CA3 regions measured as signal power (Fig. 10A) and suppression ratio (Fig. 10B, reduced by  $54 \pm 7\%$  ipsilaterally,  $56 \pm 9\%$  contralaterally, n=9), unlike that observed in the Thy1-ChR2-YFP mouse, where efficacy of seizure suppression during stimulation initially was low. Similar to the response in the Thy1 animals, seizure reduction was achieved both ipsilaterally and contralaterally after 120s of 1Hz stimulation (reduction of  $38 \pm 11\%$  and  $43 \pm 12\%$ , respectively) as well as after stimulation ( $40 \pm 11\%$  reduction on ipsilateral side only, Fig. 10A, B). Comparison of responses to oLFS in the two different transgenic mouse lines (Fig. 10C) shows that there were significant differences in the seizure reduction efficacy during the initial phase of the stimulation period and on the ipsilateral side during the second phase of stimulation. The response in the VGAT mouse was greatest at the beginning of the stimulus period but began to diminish slightly with prolonged stimulation. In contrast, the suppression in the Thy1 mouse was low initially but improved as stimulation continued, and even surpassed the response seen in the VGAT mouse (Fig. 10C). However, the overall suppressive ratio during optical stimulation was similar in both transgenic lines (Fig. 10C).

## Discussion

In this study, we used a novel optogenetic method of low-frequency stimulation in the hippocampus to investigate the role of hippocampal interneurons in LFS-mediated network

suppression in epilepsy. Neuronal activation with the excitatory construct channelrhodopsin-2 was used as an analog to an electrical stimulus, but with the advantage of cell type-specificity through genetic targeting. We showed that oLFS could effectively reduce epileptiform activity in the hippocampus. Selective activation of hippocampal interneurons induced a paradoxical excitatory bursting in the pyramidal cell network that caused entrainment and overall suppression of hyperactivity.

Electrical stimulation has been shown to be an effective method to suppress seizures by more than 85% in *in vitro* (Toprani and Durand, 2013a) and *in vivo* (Zhang *et al.*, 2009; Xu *et al.*, 2010; Rashid *et al.*, 2012; Tang and Durand, 2012) animal models and in human patients (Koubeissi *et al.*, 2013). However, it remains unclear and a subject of great debate whether the therapeutic effect results from activation of specific neural populations or from stimulation of glial cells, passing axons, or afferent inputs to the target neurons. Indeed, an electrical stimulus does not discriminate among cell types and has been shown to activate local neurons, axon terminals, and fibers of passage at similar stimulus thresholds (McIntyre and Grill, 2002), so the therapeutic effect could be due to multiple factors. By stimulating neurons via an optogenetic construct, we could locally target types of hippocampal neurons more specifically, ensuring that the resulting effect was attributed to activation of these cells and not glial cells or projections from distant neurons. Unlike electrical stimulation, optical activation of axons expressing ChR2 requires a higher stimulus intensity than for neuronal somata and dendrites (Foutz *et al.*, 2012), limiting the activation of afferent connections and passing fibers in the stimulus region that may contain ChR2. In addition, it is not known whether the effect of low frequency electrical stimulation is due to activation of pyramidal cells or inhibitory neurons. In the present study, we were able to selectively stimulate hippocampal interneurons without the use of pharmacologic inhibitors that would alter the neural network, and we observed that selective activation of these cells reduces seizure activity. Unexpectedly, the mechanism responsible for suppression even in this case appears to still involve pyramidal cell activation rather than inhibition.

As previous studies have shown that mechanisms involved in LFS suppression include both interneuron-mediated processes as well as inhibitory mechanisms following pyramidal cell excitation (Toprani and Durand, 2013a; 2013b), we initially set out to optically activate all neuronal cell types in the hippocampus using the LFS paradigm to assess LFS efficacy using an optical stimulus. The transgenic mouse line Thy1-ChR-YFP expresses the ChR2 optogenetic construct pan-neuronally, making it ideal for such an investigation. Application of oLFS *in vivo* proved to be effective at entraining neural activity in the hippocampus while reducing ongoing ictal activity by as much as 70% (Fig. 2). Histologic assessment, however, yielded a complex and unexpected expression pattern in the hippocampus (Fig. 4). Though Thy-1 expression is pan-neuronal (Barclay and Hyden, 1978), we observed relatively little ChR2-YFP expression in hippocampal pyramidal cells and rather it was detected predominantly in GABA interneurons (Figs. 4 and Fig. 5). Our *in vitro* electrophysiology studies in Thy1-ChR2-YFP brain slices, however, did show evidence of light-induced pyramidal cell depolarization (Fig. 3), indicating that a sub-population of these cells could be optically activated. We next used the VGAT-ChR2-YFP transgenic mouse line, which expresses ChR2 only in GABAergic neurons, to more specifically investigate the role of

interneurons in oLFS and rule out any concurrent activation of pyramidal neurons. Under normal conditions, optical stimuli produced a picrotoxin-sensitive IPSP response in pyramidal cells with a reversal potential of approximately  $-65$  mV (Fig. 8), similar to what has been reported with exogenously applied GABA (Ben-Ari et al., 1989). Interestingly, optical stimuli during epileptogenic conditions generated an excitatory pyramidal cell burst that resembled spontaneous bursting seen during inter-ictal epileptiform activity in the hippocampus (Perreault and Avoli, 1991) and that was also picrotoxin-sensitive (Fig. 8). While direct GABA-mediated excitation via a chloride reversal mechanism should be considered (Ben-Ari *et al.*, 2007), the fact that the reversal potential of the optical response did not change after induction of epileptiform activity makes this unlikely (Fig. 9). Rather, the intermittent network bursting caused pyramidal cells to maintain a relative hyperpolarization, likely due to a large and long-lasting AHP (Toprani and Durand, 2013b). In this setting, it is not surprising that GABA<sub>A</sub> activation would cause membrane depolarization.

It has been shown that activation of GABA<sub>A</sub> receptors induces a “shunting” current rather than a simple hyperpolarizing current that inhibits neural activity (Alger and Nicoll, 1979; Vida et al., 2006), and the  $E_{\text{GABA}}$  reversal potential may be spatially-specific (somatic vs. dendritic) and more depolarized than once thought (Gulledge and Stuart, 2003), leading to a complex role for GABA signaling that involves both cell inhibition and excitation (Andersen *et al.*, 1980; Chavas and Marty, 2003). Even when  $E_{\text{GABA}}$  is below the action potential threshold, depolarizing IPSPs in cortical pyramidal cells can facilitate neuronal firing when paired with another excitatory input, such as a glutamatergic EPSP occurring elsewhere in the cell (Gulledge and Stuart, 2003). Indeed, seizure disorders are thought to result from an imbalance between excitation and inhibition (Chang and Lowenstein, 2003), and a neural network in a state of increased excitatory synaptic input would be more likely to experience concurrent EPSP/IPSP synaptic events occurring throughout the dendritic arbor. In our experiments, we used the delayed-rectifier potassium channel blocker 4-aminopyridine (4-AP) to pharmacologically induce this imbalance as a model of epilepsy. When applied at low doses, 4-AP will induce epileptiform activity by enhancing synaptic activity in all neurons (Rutecki *et al.*, 1987). This model was chosen because all hippocampal synaptic connections remain functionally intact, making it ideal to study seizure suppression phenomena that involve both pyramidal cell- and interneuron-mediated mechanisms.

We speculate that optical stimuli in the optogenetic mouse elicited a synchronous release of GABA throughout the hippocampus in the setting of increased glutamatergic synaptic tone caused by pro-epileptogenic conditions, leading to an IPSP-mediated facilitation of excitatory inputs resulting in synchronous pyramidal cell firing. The fact that an identical response was produced by synchronously eliciting a glutamatergically-driven excitatory process through electrical stimulation (Fig. 7) underscores that optical activation of the GABAergic system produced pyramidal cell excitation in this model of epilepsy. There is significant evidence that interneuron signaling can drive synchronous pyramidal cell activity, both under normal and epileptogenic experimental conditions. It has been estimated that a single GABAergic interneuron may contact more than a thousand pyramidal neurons

(Li *et al.*, 1994; Sik *et al.*, 1995), providing a common temporal reference to a large number of cells. Interneuron networks have been implicated in generating gamma oscillations (30–90 Hz) in the cortex (Whittington *et al.*, 1995) and both gamma and theta oscillations (4–7 Hz) in the hippocampus (Cobb *et al.*, 1995; Vida *et al.*, 2006). It has also been shown that increased interneuron activity and synchronous GABA<sub>A</sub>-mediated IPSPs in pyramidal cells are correlated with inter-ictal epileptiform bursting that often precedes seizure onset (Lopantsev and Avoli, 1998; Ziburkus *et al.*, 2006), and pre-synaptic depletion of GABA<sub>A</sub> is associated with the transition toward an ictal event (Zhang *et al.*, 2012). While it is clear that inter-ictal bursting is pathologic and results from abnormal large post-synaptic depolarizations (Matsumoto, 1964), there is much debate over the potentially protective nature of this activity given recent evidence suggesting that increased neuronal spatial synchrony may be involved in the termination of seizures (Schindler *et al.*, 2007; Timofeev and Steriade, 2004). Indeed, we observed a decrease in pyramidal cell spontaneous firing that correlated to an overall stabilization and lowering of the resting membrane potential when we optically stimulated at 1Hz (Fig. 6 and Fig. 7), a frequency specifically chosen to mimic inter-ictal activity. This effect could explain, at least in part, how oLFS applied *in vivo* during electrographic seizure reduces hyperactivity.

It is important to note that while CA3 seizure suppression with electrical LFS may be due to antidromic activation of CA3 pyramidal cells, the oLFS-mediated suppression we have presented here resulted largely from orthodromic activation via a GABA<sub>A</sub>-mediated mechanism. Although there is evidence that GABA<sub>A</sub> is not necessary for suppression of activity resulting from electrical LFS applied to a white matter tract (Schiller and Bankirer, 2007; Toprani and Durand, 2013a), these studies did not investigate the potential excitatory role of GABA signaling since pyramidal neurons were stimulated directly. Since ultimately the regular activation of pyramidal neurons is responsible for network entrainment and suppression of activity, it is likely that the increased efficacy of oLFS seen in the Thy1 model compared to VGAT (Fig. 10) was due to the additional ChR2 expression, albeit small, in the hippocampal pyramidal cells, facilitating excitation and synchronization with the optical stimulus. Regardless, it is clear that excitation of the GABAergic system in the hippocampus can drive LFS-mediated epilepsy suppression, and a better understanding of how interneurons influence and interact with epileptogenic pyramidal cell networks will aid in the development of better seizure suppression therapies.

## Acknowledgments

This work was funded by the National Institutes of Health (NINDS) Grant# 5R01NS040785-04 and the Case Western Reserve University MSTP fellowship (NIH T32 GM007250).

## References

- Alger BE, Nicoll RA. GABA-mediated biphasic inhibitory responses in hippocampus. *Nature*. 1979; 281:315–317. [PubMed: 551280]
- Andersen P, Dingledine R, Gjerstad L, Langmoen IA, Laursen AM. Two different responses of hippocampal pyramidal cells to application of gamma-amino butyric acid. *The Journal of Physiology*. 1980; 305:279–296. [PubMed: 7441554]

- Arenkiel BR, Peca J, Davison IG, Feliciano C, Deisseroth K, Augustine GJ, et al. In vivo light-induced activation of neural circuitry in transgenic mice expressing channelrhodopsin-2. *Neuron*. 2007; 54:205–218. [PubMed: 17442243]
- Barclay AN, Hyden H. Localization of the Thy-1 Antigen in Rat Brain and Spinal Cord by Immunofluorescence. *J Neurochem*. 1978; 31:1375–1391. [PubMed: 45112]
- Ben-Ari Y, Cherubini E, Corradetti R, Gaiarsa JL. Giant synaptic potentials in immature rat CA3 hippocampal neurones. *The Journal of Physiology*. 1989; 416:303–325. [PubMed: 2575165]
- Ben-Ari Y, Gaiarsa J-L, Tyzio R, Khazipov R. GABA: a pioneer transmitter that excites immature neurons and generates primitive oscillations. *Physiol Rev*. 2007; 87:1215–1284. [PubMed: 17928584]
- Boyden ES, Zhang F, Bamberg E, Nagel G, Deisseroth K. Millisecond-timescale, genetically targeted optical control of neural activity. *Nat Neurosci*. 2005; 8:1263–1268. [PubMed: 16116447]
- Bragin A, Wilson CL, Engel J. Rate of interictal events and spontaneous seizures in epileptic rats after electrical stimulation of hippocampus and its afferents [Internet]. *Epilepsia*. 2002; 43 (Suppl 5):81–85. Available from: <http://onlinelibrary.wiley.com/doi/10.1046/j.1528-1157.43.s.5.22.x.full>. [PubMed: 12121300]
- Chang BS, Lowenstein DH. *Epilepsy*. *N Engl J Med*. 2003; 349:1257–1266. [PubMed: 14507951]
- Chavas J, Marty A. Coexistence of excitatory and inhibitory GABA synapses in the cerebellar interneuron network. *J Neurosci*. 2003; 23:2019–2031. [PubMed: 12657660]
- Chiang C-C, Lin C-CK, Ju M-S, Durand DM. High frequency stimulation can suppress globally seizures induced by 4-AP in the rat hippocampus: An acute in vivo study. *Brain Stimul*. 2013; 6:180–189. [PubMed: 22621942]
- Chiang CC, Ladas TP, Gonzalez-Reyes LE, Durand DM. Seizure suppression by high frequency optogenetic stimulation using in vitro and in vivo animal models of epilepsy. *Brain Stimul*. 2014; 7:890–899. [PubMed: 25108607]
- Chow BY, Han X, Dobry AS, Qian X, Chuong AS, Li M, et al. High-performance genetically targetable optical neural silencing by light-driven proton pumps. *Nature*. 2010; 463:98–102. [PubMed: 20054397]
- Cobb SR, Buhl EH, Halasy K, Paulsen O, Somogyi P. Synchronization of neuronal activity in hippocampus by individual GABAergic interneurons. *Nature*. 1995; 378:75–78. [PubMed: 7477292]
- Fisher R, Salanova V, Witt T, Worth R, Henry T, Gross R, et al. Electrical stimulation of the anterior nucleus of thalamus for treatment of refractory epilepsy. *Epilepsia*. 2010; 51:899–908. [PubMed: 20331461]
- Foutz TJ, Arlow RL, McIntyre CC. Theoretical principles underlying optical stimulation of a channelrhodopsin-2 positive pyramidal neuron. *J Neurophysiol*. 2012; 107:3235–3245. [PubMed: 22442566]
- Gonzalez-Reyes LE, Ladas TP, Chiang CC, Durand DM. TRPV1 antagonist capsazepine suppresses 4-AP-induced epileptiform activity in vitro and electrographic seizures in vivo. *Exp Neurol*. 2013 Dec; 250:321–32. [PubMed: 24145133]
- Gulledge AT, Stuart GJ. Excitatory Actions of GABA in the Cortex. *Neuron*. 2003; 37:299–309. [PubMed: 12546824]
- Jobst BC, Darcey TM, Thadani VM, Roberts DW. Brain stimulation for the treatment of epilepsy. *Epilepsia*. 2010; 51 (Suppl 3):88–92. [PubMed: 20618409]
- Koubeissi MZ, Kahrman E, Syed TU, Miller J, Durand DM. Low-frequency electrical stimulation of a fiber tract in temporal lobe epilepsy. *Ann Neurol*. 2013; 74:223–231. [PubMed: 23613463]
- Krook-Magnuson E, Armstrong C, Oijala M, Soltesz I. On-demand optogenetic control of spontaneous seizures in temporal lobe epilepsy. *Nat Rev Neurosci*. 2013; 4:1376.
- Lévesque M, Salami P, Behr C, Avoli M. Temporal lobe epileptiform activity following systemic administration of 4-aminopyridine in rats. *Epilepsia*. 2013; 54:596–604. [PubMed: 23521339]
- Li XG, Somogyi P, Ylinen A, Buzsáki G. The hippocampal CA3 network: an in vivo intracellular labeling study. *J Comp Neurol*. 1994; 339:181–208. [PubMed: 8300905]
- Lopantsev V, Avoli M. Participation of GABAA-mediated inhibition in ictallike discharges in the rat entorhinal cortex. *Journal of Neurophysiology*. 1998; 79:352–360. [PubMed: 9425204]

- Matsumoto H. Intracellular events during the activation of cortical epileptiform discharges. *Electroencephalogr Clin Neurophysiol*. 1964; 17:294–307. [PubMed: 14207697]
- McIntyre CC, Grill WM. Extracellular stimulation of central neurons: influence of stimulus waveform and frequency on neuronal output. *Journal of Neurophysiology*. 2002; 88:1592–1604. [PubMed: 12364490]
- Morrell MJ. Responsive cortical stimulation for the treatment of medically intractable partial epilepsy. *Neurology*. 2011; 77:1295–1304. [PubMed: 21917777]
- Paz JT, Davidson TJ, Frechette ES, Delord B, Parada I, Peng K, et al. Closed-loop optogenetic control of thalamus as a tool for interrupting seizures after cortical injury. *Nat Neurosci*. 2013; 16(1):64–70. [PubMed: 23143518]
- Perreault P, Avoli M. Effects of low concentrations of 4-aminopyridine on CA1 pyramidal cells of the hippocampus. *Journal of Neurophysiology*. 1989; 61:953–970. [PubMed: 2566657]
- Perreault P, Avoli M. Physiology and pharmacology of epileptiform activity induced by 4-aminopyridine in rat hippocampal slices. *Journal of Neurophysiology*. 1991; 65:771–785. [PubMed: 1675671]
- Rashid S, Pho G, Czigler M, Werz MA, Durand DM. Low frequency stimulation of ventral hippocampal commissures reduces seizures in a rat model of chronic temporal lobe epilepsy. *Epilepsia*. 2012; 53:147–156. [PubMed: 22150779]
- Rutecki PA, Lebeda FJ, Johnston D. 4-Aminopyridine produces epileptiform activity in hippocampus and enhances synaptic excitation and inhibition. *Journal of Neurophysiology*. 1987; 57:1911–1924. [PubMed: 3037040]
- Schiller Y, Bankirer Y. Cellular Mechanisms Underlying Antiepileptic Effects of Low- and High-Frequency Electrical Stimulation in Acute Epilepsy in Neocortical Brain Slices In Vitro. *J Neurophysiol*. 2007; 97:1887–902. [PubMed: 17151229]
- Schindler K, Elger CE, Lehnertz K. Increasing synchronization may promote seizure termination: evidence from status epilepticus. *Clin Neurophysiol*. 2007; 118:1955–1968. [PubMed: 17644031]
- Sik A, Penttonen M, Ylinen A, Buzsáki G. Hippocampal CA1 interneurons: an in vivo intracellular labeling study. *J Neurosci*. 1995; 15:6651–6665. [PubMed: 7472426]
- Sunderam S, Gluckman B, Reato D, Bikson M. Toward rational design of electrical stimulation strategies for epilepsy control. *Epilepsy Behav*. 2010; 17:6–22. [PubMed: 19926525]
- Tang Y, Durand DM. A novel electrical stimulation paradigm for the suppression of epileptiform activity in an in vivo model of mesial temporal lobe status epilepticus. *Int J Neural Syst*. 2012; 22:1250006. [PubMed: 23627622]
- Tawfik VL, Chang S-Y, Hitti FL, Roberts DW, Leiter JC, Jovanovic S, et al. Deep brain stimulation results in local glutamate and adenosine release: investigation into the role of astrocytes. *Neurosurgery*. 2010; 67:367–375. [PubMed: 20644423]
- Timofeev I, Steriade M. Neocortical seizures: initiation, development and cessation. *Neuroscience*. 2004; 123:299–336. [PubMed: 14698741]
- Toprani S, Durand DM. Fiber tract stimulation can reduce epileptiform activity in an in-vitro bilateral hippocampal slice preparation. *Exp Neurol*. 2013a; 240:28–43. [PubMed: 23123405]
- Toprani S, Durand DM. Long-lasting hyperpolarization underlies seizure reduction by low frequency deep brain electrical stimulation. *J Physiol*. 2013b; 591 (Pt 22):5765–90. [PubMed: 23981713]
- Vida I, Bartos M, Jonas P. Shunting inhibition improves robustness of gamma oscillations in hippocampal interneuron networks by homogenizing firing rates. *Neuron*. 2006; 49:107–117. [PubMed: 16387643]
- Whittington MA, Traub RD, Jefferys JG. Synchronized oscillations in interneuron networks driven by metabotropic glutamate receptor activation. *Nature*. 1995; 373:612–615. [PubMed: 7854418]
- Wiebe S, Blume WT, Girvin JP, Eliasziw M. Effectiveness and Efficiency of Surgery for Temporal Lobe Epilepsy Study Group. . A randomized, controlled trial of surgery for temporal-lobe epilepsy. *N Engl J Med*. 2001; 345:311–318. [PubMed: 11484687]
- Woodson W, Nitecka L, Ben-Ari Y. Organization of the GABAergic system in the rat hippocampal formation: a quantitative immunocytochemical study. *J Comp Neurol*. 1989; 280:254–271. [PubMed: 2925894]

- Wykes RC, Heeroma JH, Mantoan L, Zheng K, Macdonald DC, Deisseroth K, et al. Optogenetic and Potassium Channel Gene Therapy in a Rodent Model of Focal Neocortical Epilepsy. *Sci Transl Med*. 2012; 4(161):161ra152.
- Xu Z-H, Wu D-C, Fang Q, Zhong K, Wang S, Sun H-L, et al. Therapeutic time window of low-frequency stimulation at entorhinal cortex for amygdaloid-kindling seizures in rats. *Epilepsia*. 2010; 51:1861–1864. [PubMed: 20662893]
- Yang L-X, Jin C-L, Zhu-Ge Z-B, Wang S, Wei E-Q, Bruce IC, et al. Unilateral low-frequency stimulation of central piriform cortex delays seizure development induced by amygdaloid kindling in rats. *Neuroscience*. 2006; 138:1089–1096. [PubMed: 16427743]
- Zhang F, Wang L-P, Brauner M, Liewald JF, Kay K, Watzke N, et al. Multimodal fast optical interrogation of neural circuitry. *Nature*. 2007; 446:633–639. [PubMed: 17410168]
- Zhang M, Ladas TP, Qiu C, Shivacharan RS, Gonzalez-Reyes LE, Durand DM. Propagation of epileptiform activity can be independent of synaptic transmission, gap junctions, or diffusion and is consistent with electrical field transmission. *J Neurosci*. 2014; 34:1409–1419. [PubMed: 24453330]
- Zhang S-H, Sun H-L, Fang Q, Zhong K, Wu D-C, Wang S, et al. Low-frequency stimulation of the hippocampal CA3 subfield is anti-epileptogenic and anti-ictogenic in rat amygdaloid kindling model of epilepsy. *Neuroscience Letters*. 2009; 455:51–55. [PubMed: 19429105]
- Zhang ZJ, Koifman J, Shin DS, Ye H, Florez CM, Zhang L, et al. Transition to seizure: ictal discharge is preceded by exhausted presynaptic GABA release in the hippocampal CA3 region. *J Neurosci*. 2012; 32:2499–2512. [PubMed: 22396423]
- Zhao S, Ting JT, Atallah HE, Qiu L, Tan J, Gloss B, et al. Cell type specific channelrhodopsin-2 transgenic mice for optogenetic dissection of neural circuitry function. *Nat Meth*. 2011; 8:745–752.
- Ziburkus J, Cressman JR, Barreto E, Schiff SJ. Interneuron and pyramidal cell interplay during in vitro seizure-like events. *Journal of Neurophysiology*. 2006; 95:3948–3954. [PubMed: 16554499]



### Highlights

- Low frequency optical stimulation significantly suppresses epileptiform activity *in vitro* and *in vivo*.
- Selective optical activation of hippocampal interneurons at low frequency suppresses epileptiform activity in the hippocampus.
- Activation of GABA interneurons causes entrainment of hippocampal CA3 pyramidal cells by a GABA<sub>A</sub> mediated mechanism.

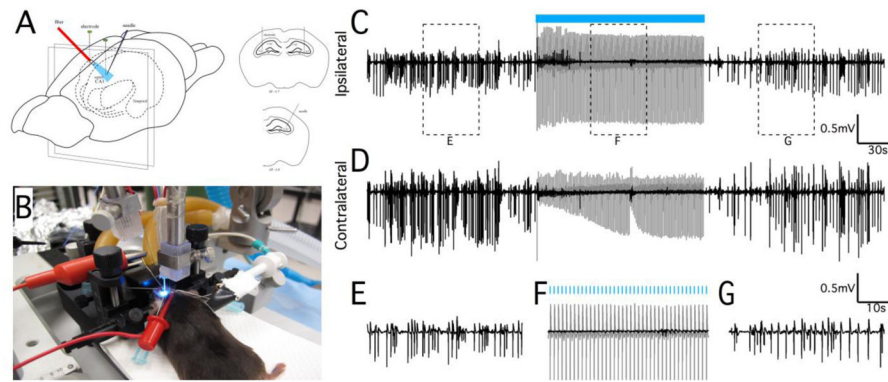


**Figure 1.**

Optical stimulation at 1Hz can suppress *in vivo* epileptiform activity. **(A)** Schematic representation of *in vivo* optical stimulation in the mouse hippocampus. Actual experimental preparation is shown in **(B)**. Recording electrodes were positioned bilaterally in the septal CA3 regions. Epileptiform activity was induced by unilateral bolus injection of 40mM 4-AP, and an optical fiber was positioned to maximally illuminate the dorsal hippocampus near the injection site. Neural recordings from electrodes positioned in the ipsilateral **(C)** and contralateral **(D)** septal CA3 regions showing hippocampal seizure activity before, during, and after a 2 min period of optical stimulation at 1Hz (indicated by blue bar). Stimulation was only applied to the site of 4-AP injection (ipsilateral site), but reduction of epileptiform activity occurred bilaterally. **(E–G)** Magnification of the regions identified in **(C)** to show the seizure and suppressed activity in greater detail. Note that the optical evoked potential during the stimulation period (gray traces) was removed from these recordings by template subtraction (black trace, see Methods). Stimulation trials in wild-type control animals did not elicit an optical evoked potential and had no effect on epileptiform activity (data not shown).

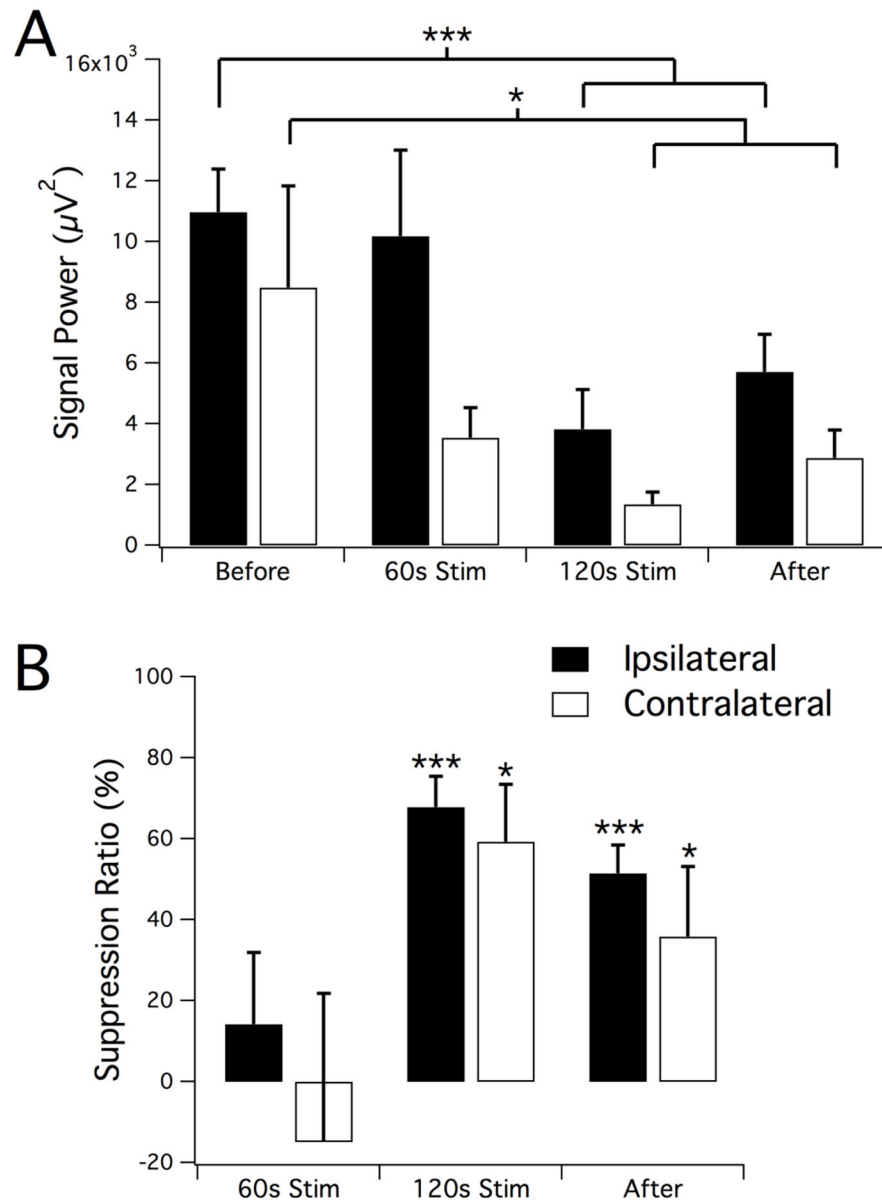


**Figure 2.** Reduction of ictal activity in response to oLFS. Signal power (**A**) and calculated suppression ratio (**B**) from ipsilateral and contralateral recordings in the intervals before, during, and after the optical stimulation period. A significant reduction in seizure activity was observed during the second minute of stimulation as well as an after-effect of continued suppression of activity in the ipsilateral location. Results are the mean  $\pm$  SEM,  $n=7$ , \* $P<0.05$ , \*\*\* $P<0.001$ , paired t-test.

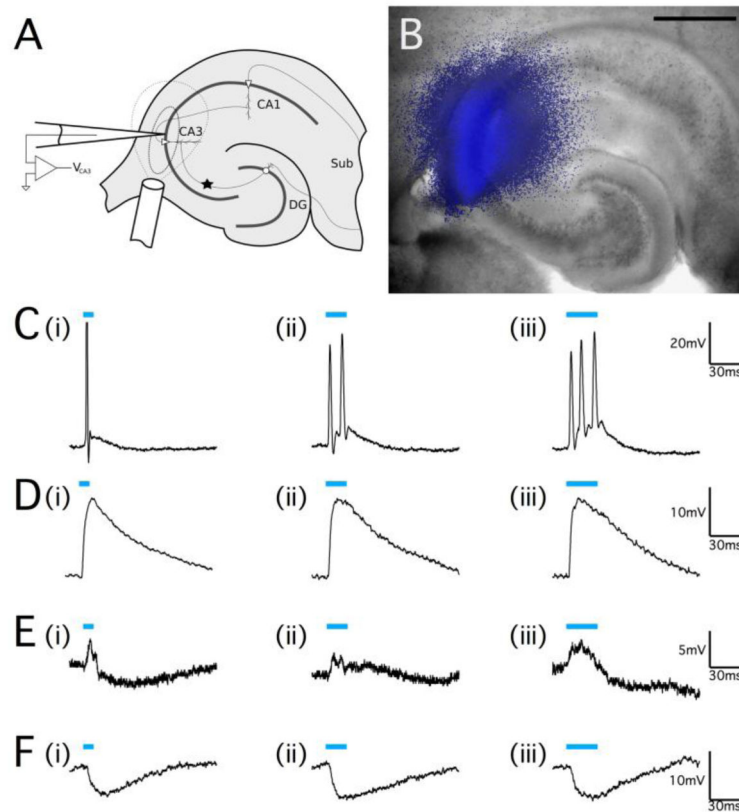


**Figure 3.**

Optical stimulation of ChR2 can cause both excitation and inhibition in the hippocampus. (A) Schematic representation of optical stimulation of hippocampal slices. The star indicates the location of mossy fiber monopolar stimulation to elicit an orthodromic response in CA3. The 200 μm diameter optical fiber was positioned directly over the CA3 pyramidal cell region, and the areas marked by the dashed lines indicate the spatial extent of the optical stimulus (inner line indicating the area of most intense illumination close to the fiber output) as determined by image capture of the illumination (B) of the *in vitro* transverse hippocampal slice. Scale bar, 500 μm. (C–F) Whole-cell patch clamp recordings of neurons in the pyramidal cell layer of the CA3 region of the hippocampus from juvenile Thy1-ChR2 mice. (C) Pulsed optical stimulation using 473nm light (indicated by blue bars) at a power of 20mW applied for 10ms (C, i), 20ms (C, ii), and 30ms (C, iii) was able to reliably elicit action potential responses. (D) Optical stimulation of a different cell at the same power and pulse durations that caused a large cell depolarization but did not elicit action potential firing. (E) A cell that responded to optical stimulus pulses with an excitation-inhibition response. (F) A pyramidal neuron that exhibited a pure hyperpolarization response to optical pulse stimulation without any depolarization. The resting membrane potential for all cells was –55mV to –60mV.

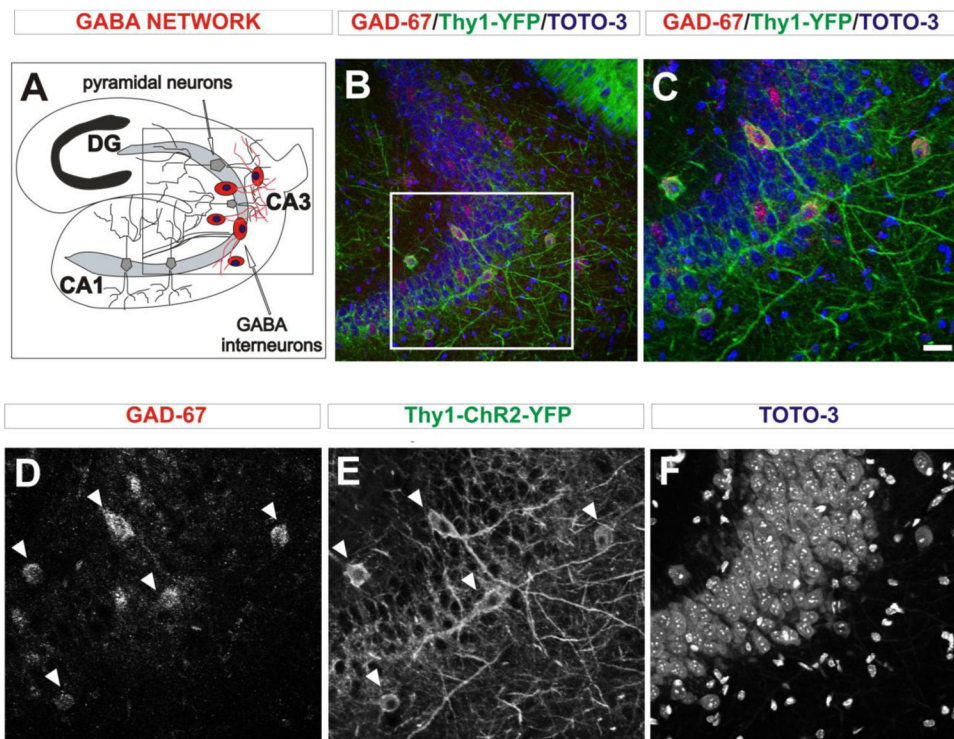


**Figure 4.** GAD-67 immunostaining in Thy1-ChR2-YFP hippocampal sections in P14 mice. (A) Diagram showing the localization of the GABA interneuron network in the CA3 region of the hippocampus. (B) Panoramic view of CA3 shows interneurons co-expressing YFP and GABAergic marker GAD-67. (C) Magnified view of the region indicated in B to show the YFP-positive cells in CA3 in greater detail. (D–F) Single image channels for GAD-67 (D), YFP (E), and TOTO-3 (F) that comprise the merged image in C. Cells co-expressing GAD-67 (D) and YFP (E) are indicated by arrowheads. The densely clustered pyramidal cells in this region of the hippocampus are shown by the TOTO-3 nuclear stain (F). Scale bar: 20 $\mu$ m.

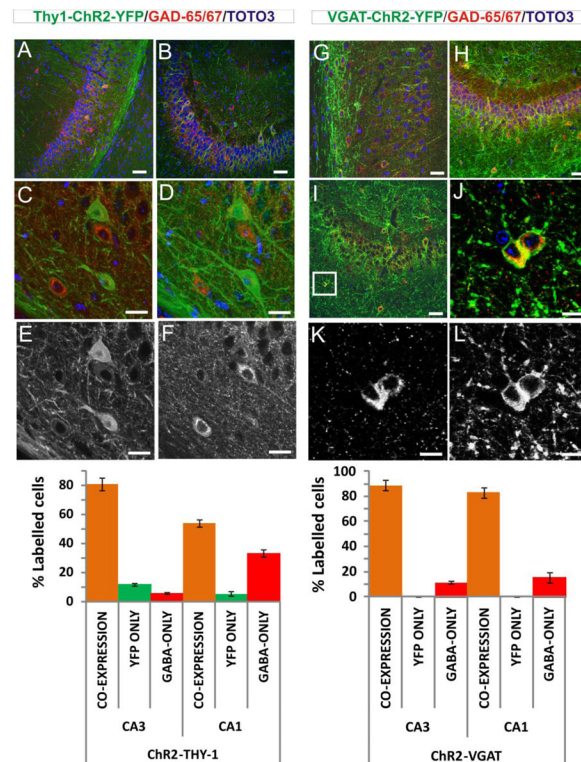


**Figure 5.**

Immunostaining and cell count summary for GABA interneurons in Thy1- and VGAT-ChR2-YFP hippocampal sections.

- (A) Thy1-ChR2-YFP mouse (P14), panoramic view of CA1 showing two cells in the pyramidal cell layer co-expressing YFP and GAD-65/67 markers, which indicates that are GABA cells positive for ChR2. Note that some cells off the pyramidal cell layer only express GAD-65/67. Scale Bar 50  $\mu$ m.
- (B) Thy1-ChR2-YFP adult mouse (P100), panoramic view of CA3 showing that most cells expressing YFP also express GAD-65/67. Scale Bar 50  $\mu$ m.
- (C) Thy1-ChR2-YFP mouse (P100), example of two pyramidal cells expressing YFP but not GAD-65/67. This shows that ChR2 in the Thy-1 line is also express in pyramidal (excitatory) cells, which do not stain for GAD-65/67. The image corresponds to a single plane picture. Scale Bar 20  $\mu$ m.
- (D) Thy1-ChR2-YFP mouse, corresponding to a projection within 30  $\mu$ m depth of the same image as in (C). Scale Bar 20  $\mu$ m.
- (E) Thy1-ChR2-YFP mouse, same image as in (C) in the green YFP channel showing pyramidal cells positive to YFP. Scale Bar 20  $\mu$ m.
- (F) Thy1-ChR2-YFP mouse, same image as in (C) in the red GAD-65/67 channel showing GABA cells positive to GAD-65/67. Scale Bar 20  $\mu$ m.
- (G) VGAT-ChR2-YFP mouse (P14), panoramic view of CA1 showing that most cells in the pyramidal cell layer co-expressing YFP and GAD-65/67 markers, which indicates that are GABA interneurons positive for ChR2. Scale Bar 50  $\mu$ m.

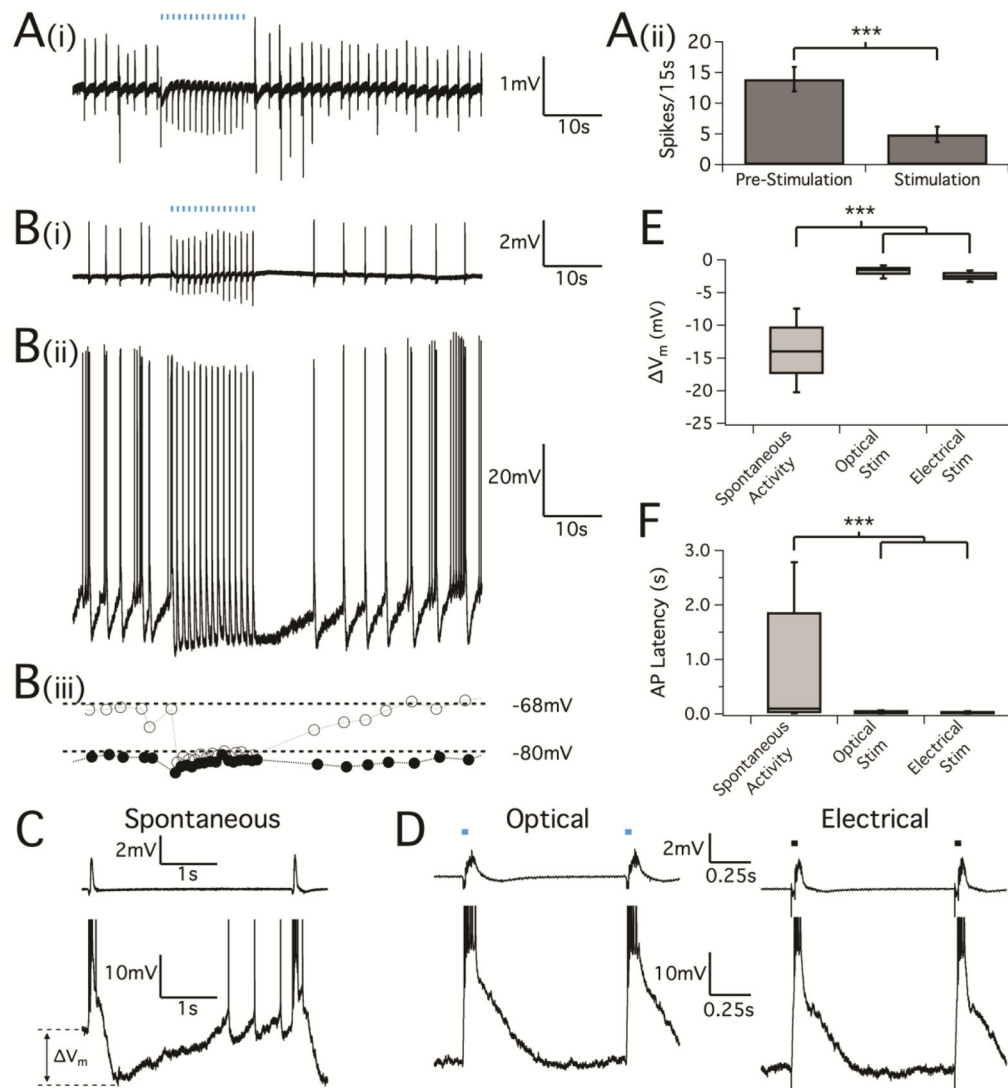
**(H)** VGAT-ChR2-YFP mouse (P14), panoramic view of CA3 showing that most cells in the pyramidal cell layer co-expressing YFP and GAD-65/67 markers, which indicates that are GABA interneurons positive for ChR2. Scale Bar 50  $\mu$ m.

**(I)** VGAT-ChR2-YFP mouse (P100), panoramic view of CA3 showing that most cells in the pyramidal cell layer co-expressing YFP and GAD-65/67 markers. Scale Bar 50  $\mu$ m. The image includes a square area that was selected for enlargement in **(H)**.

**(J)** VGAT-ChR2-YFP mouse, magnified view of two cells co-expressing YFP and GAD-65/67. Scale Bar 20  $\mu$ m

**(K)** VGAT-ChR2-YFP mouse, same as **(I)** for red GAD-65/67 channel. Scale Bar 20  $\mu$ m.

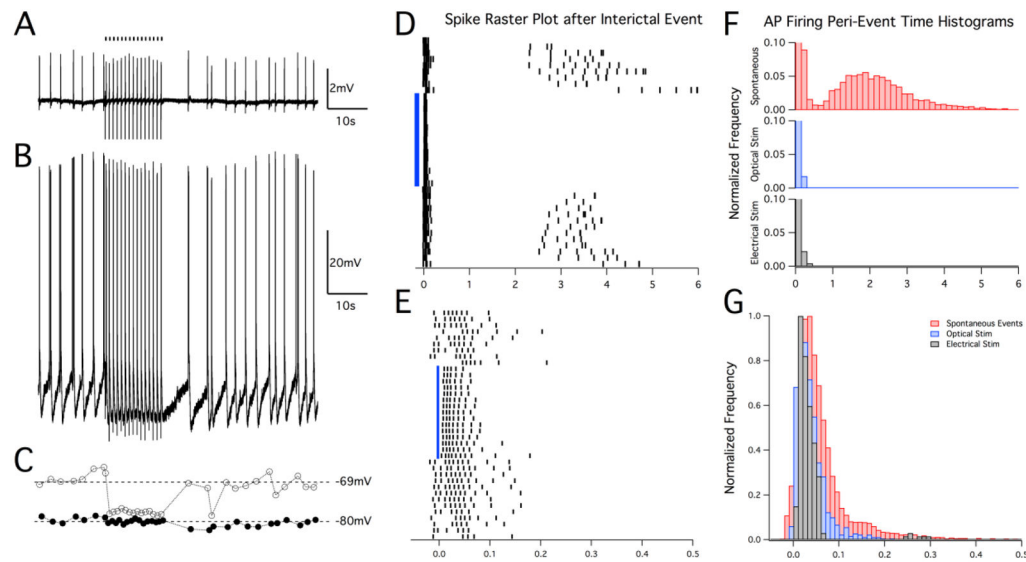
**(L)** VGAT-ChR2-YFP mouse, same as **(J)** for green YFP channel. Scale Bar 20  $\mu$ m.

**Figure 6.**

LFS entrainment of interictal bursting by GABA<sub>A</sub> activation from optical stimulation. Transverse hippocampal slices undergoing spontaneous interictal bursting were stimulated with optical pulses at a frequency of 1Hz. **(A, i)** Field potential recordings in CA3 of adult mice (P90) showing neural activity was evoked by optical stimulation and **(A, ii)** caused the reduction of inter-ictal spiking ( $p < 0.001$ , paired t test,  $n = 18$ ). **(B, i)** Field potential recordings in CA3 of juvenile mice (P14-16) showing neural activity followed by optically-evoked potentials which is similar to what has shown in adult mice. **(B, ii)** Corresponding intracellular activity using sharp electrodes from a nearby CA3 pyramidal cell. Blue bars indicate optical pulses (10ms). Note that the length of the stimulus bars is not to scale. **(B, iii)** Plot of the voltage immediately preceding a bursting event (gray open circles) together with the minimum voltage between events (black circles). **(C)** Cellular behavior as recorded by sharp electrodes during spontaneous inter-ictal activity showing a burst of action potentials that corresponds to the field potential event, followed by a hyperpolarization and gradual return to the resting membrane potential before the next spontaneous burst. As the

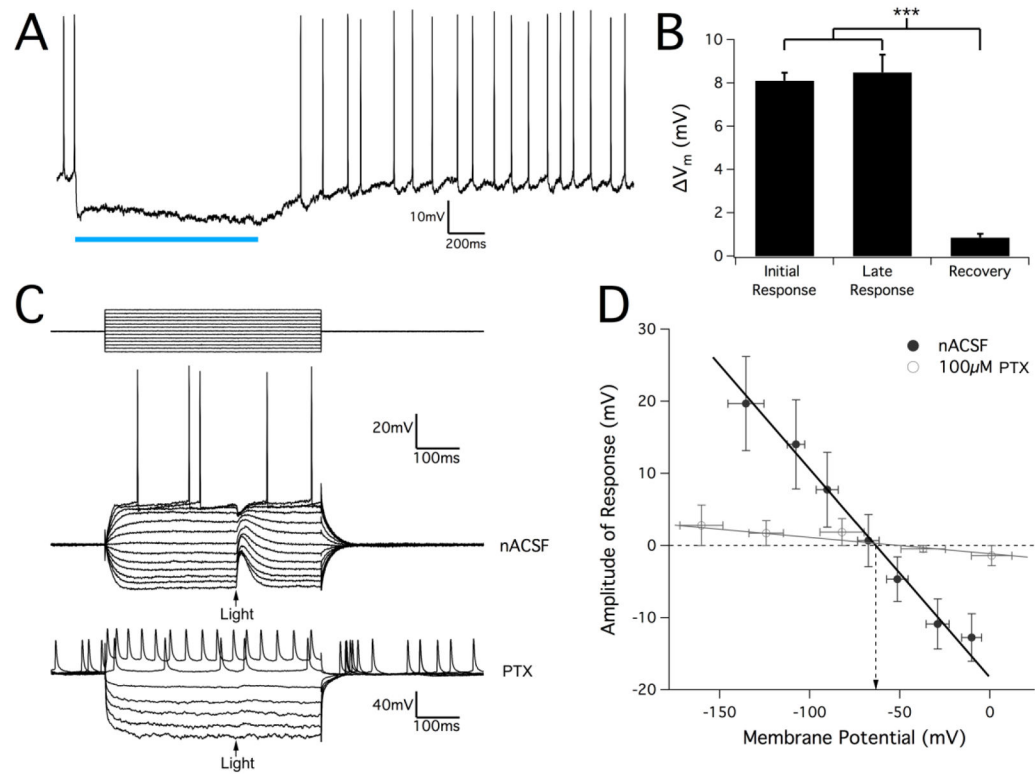


cell depolarizes back to rest, spontaneous action potentials often precede the next epileptiform burst. **(D)** Cellular behavior during oLFS (left) and electrical LFS applied to the mossy fibers (right). Blue and black bars (again not to scale) indicate the optical and electrical stimuli, respectively. **(E)** Box-and-whisker plot of the change in membrane voltage induced by spontaneous and evoked bursting events. While the cell membrane potential varies widely during spontaneous inter-ictal activity, membrane voltage remained low in between evoked bursts during the stimulus periods.  $P < 0.001$ , one-way ANOVA. **(F)** Box-and-whisker plots of AP spike timing after spontaneous and evoked bursting events. During low frequency stimulus periods were marked by a reduction of cellular inter-event action potential activity.  $P < 0.001$ , Kolmogorov-Smirnov test of distributions.



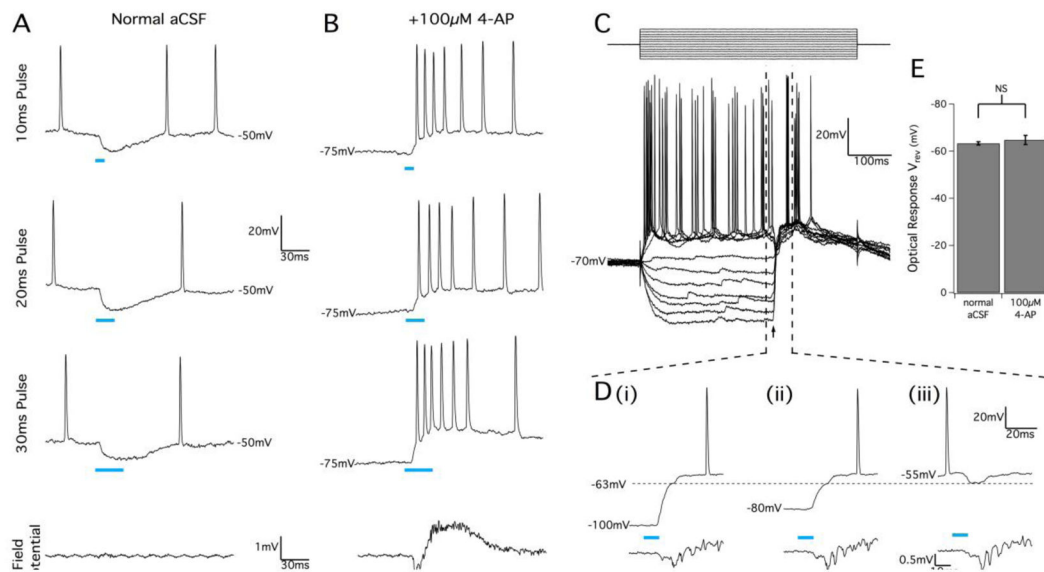
**Figure 7.**

Sculpting of neuronal membrane potential and firing behavior is similar for optical and electrical LFS paradigms. (A) Field potential recording in the CA3 region of juvenile hippocampal slices and corresponding cellular recording by sharp electrodes (B) during 4-AP epileptiform activity showing entrainment of activity to 1Hz electrical LFS in the mossy fibers in a similar manner as with optical stimulation (Fig. 6B). (C) Plot of the voltage immediately preceding a bursting event (gray open circles) together with the minimum voltage between events (black circles). (D) Example raster plot of cell firing in response to spontaneous and optically-evoked events. Events are aligned at  $t = 0$ , which correlates to the initial negative phase of the field potential burst. Events that were elicited by optical stimulation at 1 Hz are indicated by the blue bar. Cell firing that develops after the initial burst can be seen for spontaneous events. This behavior is shown in (F) where spike times after field bursting are summarized for each condition. For both optical and electrical LFS trials (1 Hz), any spontaneous AP firing beyond the initial burst is inhibited, thus sculpting the 1s period in between stimuli. Note that the vertical axis is expanded to better highlight the events that occurred after the initial AP burst. (E) Magnified time-scale of the raster plot in (D) to illustrate the regularity of spiking entrainment in response to the optical stimulus (blue bar, aligned at actual stimulus time  $t = 0$ ). Cell firing during spontaneous inter-ictal events occurs more randomly before and after the optical stimulus period than it does when evoked by optical stimuli. (G) AP firing histogram with expanded time-scale to highlight cell firing behavior during the initial burst event. Both optical and electrical stimulation produced similar burst responses that occurred earlier and over a shorter period than those observed in response to spontaneous inter-ictal activity.



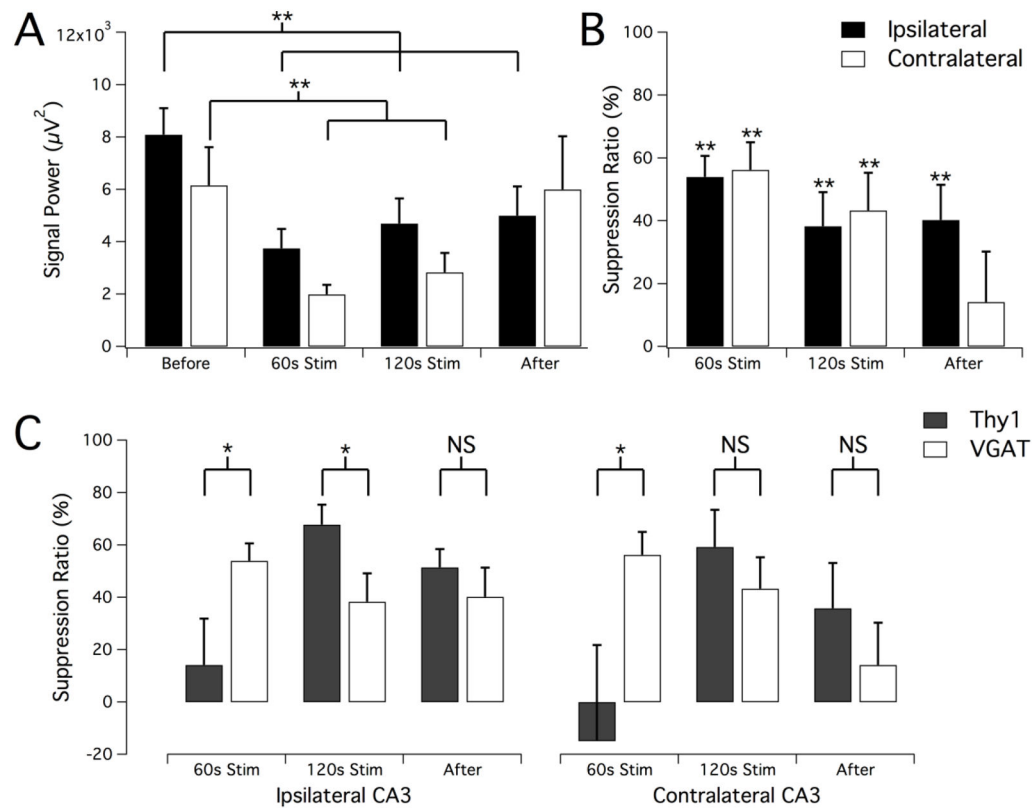
**Figure 8.**

Optical response in juvenile VGAT hippocampal slices is GABA<sub>A</sub>-mediated and causes pyramidal cell hyperpolarization in normal conditions. **(A)** Hyperpolarization response in pyramidal cells stimulated with a 1s sustained optical pulse. Spontaneous cell firing was completely inhibited during the optical stimulus. **(B)** Measurement of the magnitude of optically-induced change in membrane potential from hippocampal interneuron activation. Though membrane voltage often continued to hyperpolarize slightly, the amount of cell hyperpolarization did not change significantly over the course of the stimulus pulse. After optical stimulation, cells fully recovered to their baseline resting membrane potential. Results are mean  $\pm$  SEM,  $n=27$ .  $P<0.001$ , one-way ANOVA. **(C)** Example pyramidal cell response to a 10ms optical pulse stimulus during a series of hyperpolarizing and depolarizing injected current pulses (top traces). Optical stimulus is marked by an arrow. The stimulus protocol was repeated after applying the GABA<sub>A</sub>-blocker PTX (100 $\mu$ M), which completely eliminated any optical response. **(D)** Amplitude of optical response was measured and plotted against the membrane potential for each current pulse in order to determine the reversal potential for the optical response. After linear regression, the potential at a zero-response was calculated to be at  $-63.3\pm 0.70$  mV (mean  $\pm$  SEM,  $n=23$ , data point error bars represent SD). In 100 $\mu$ M PTX conditions, response amplitudes were nearly zero for all membrane voltages with no clear reversal potential that could be identified.



**Figure 9.**

GABA<sub>A</sub> activation by optical stimulation of juvenile VGAT slices causes pyramidal cell excitation in 4-AP conditions. **(A)** Pyramidal cell response to optical stimuli before bath application of 4-AP showing membrane hyperpolarization after 10 ms, 20 ms, and 30 ms optical pulses. Simultaneous field potential recordings in the same location (bottom trace) show no detectable population response to the optical pulse. **(B)** In the presence of 100µM 4-AP, optical stimulus pulses produced membrane depolarization and bursts of action potential firing that correlated with an optically-evoked population response detected in a nearby extracellular recording electrode. **(C)** Patch-clamp mode injected current pulse protocol (top) with 10 ms optical pulse (arrow) during 4-AP application. Optical stimulus produced a very large depolarization response at low membrane potential, but still produced hyperpolarization when the membrane was clamped above -60 mV. This is highlighted in **(D)** which shows a magnified view of the marked region in **(C)** to illustrate how optical stimuli produced an initial membrane response with a reversal potential of approximately -63 mV (horizontal dotted line), as before 4-AP application. Cells showed two phases of depolarization when the membrane voltage started at very hyperpolarized potentials **(D, i)** and **(D, ii)**, and action potential bursting in response to optical stimuli occurred during the second depolarization phase. Field potential recordings (bottom traces) confirmed that pyramidal cell bursting correlated with optically-evoked population bursting. **(E)** Summary of optical response reversal potentials in normal and 4-AP conditions. Results are mean ± SEM, P=0.394, Student's t-test.

**Figure 10.**

LFS optical suppression of epileptiform activity *in vivo* by driving solely hippocampal interneurons. **(A)** Signal power calculated before, during, and after 2-minute 1Hz optical stimulation of adult VGAT mice during ongoing electrographic seizure. Data is shown for both the ipsilateral and contralateral recording sites. Statistically significant reduction in signal power as compared to baseline was observed ipsilaterally in all measurement periods as well as contralaterally during stimulation. **(B)** Suppression ratio comparison of measurement periods, showing a 40%–60% reduction in seizure activity as a result of LFS of Chr2-expressing interneurons. **(C)** Summary of responses to oLFS to compare suppression efficacy in the Thy1- and VGAT-driven transgenic mouse lines. While stimulation in VGAT animals produced more seizure reduction than in Thy1 animals at the beginning of stimulus trials, the amount of seizure suppression that could be achieved with prolonged stimulation was greater in Thy1 animals. Results are mean  $\pm$  SEM (n=7 Thy1, n=9 VGAT). \*P 0.05, \*\*P<0.01, Student's t-test.